Applied Catalysis B: Environmental 84 (2008) 94–99

Contents lists available at ScienceDirect

Applied Catalysis B: Environmental

journal homepage: www.elsevier.com/locate/apcatb

Antibacterial activity of thin-film photocatalysts based on metal-modified TiO_2 and TiO_2:In_2O_3 nanocomposite

E.V. Skorb [a,*], L.I. Antonouskaya [b], N.A. Belyasova [b], D.G. Shchukin [c], H. Möhwald [c], D.V. Sviridov [a]

[a] Institute for Physico-Chemical Problems of Belarusian State University, Leningradskaya 14, 220030 Minsk, Belarus
[b] Belarusian State Technological University, Minsk, Belarus
[c] Max Planck Institute of Colloids and Interfaces, Potsdam, Germany

ARTICLE INFO

Article history:
Received 28 October 2007
Received in revised form 10 March 2008
Accepted 11 March 2008
Available online 21 March 2008

Keywords:
Antibacterial activity
Photocatalysis
TiO_2

ABSTRACT

Photoinduced bactericidal activity of nanostructured TiO_2 and TiO_2:In_2O_3 films and the effect of deposition of silver and bimetallic Ag/Ni nanoparticles on the pathophysiological properties of titania films were investigated. The antimicrobic activity of the films was assessed against *Psedomonas fluorescens* B-22 (gram-negative bacterium) and *Lactococcus lactis* ssp. lactis 411 (gram-positive bacterium). The silver-modified TiO_2 film demonstrates the highest photobiocide efficiency, enhancing the bactericidal activity of UV light ca. 71-fold, that results from radical improvement of microorganism adsorption and suppression of recombination of photoproduced charge carriers. Higher inactivation rate observed for *P. fluorescens* as compared to *L. lactis* can be explained in terms of comparative morphologies of the cell envelops of gram-negative and gram-positive microorganisms and the resistance of their outer membranes to the reactive oxygen species generated by photocatalytic reactions.

1. Introduction

Since the successful demonstration of the possibility of TiO_2-assisted photoinduced water cleavage by Fujishima and Honda in the early 1970s [1], TiO_2 photocatalysis has attracted great attention as a promising method of water and air cleaning [2–7] because highly active radical species produced at TiO_2 surface under UV irradiation (hydroxyl radicals generated by photoholes from the TiO_2 valence band and superoxide ions formed due to interaction of photoelectrons from conduction band with molecular oxygen) can participate in the series of oxidation reactions resulting in the destruction of organic contaminants [4,8] that leads, in the limit, to their mineralization. Being strong oxidants, the reactive oxygen species generated by the TiO_2 photocatalytic reactions also cause various damages to microorganisms ensuring their rapid inactivation. Since the pioneer work of Matsunaga et al. [9] reported for the first time the microbiocide effect of the platinised TiO_2, research work on TiO_2-assisted photocatalytic killing has been intensively conducted on a wide spectrum of pathogenic microorganisms including bacteria, viruses, fungi and algae. These disinfection studies were carried out, on the one hand, to establish the basic photokilling mechanisms or to identify the effective disinfection factors [9–12] and, on the other hand, to investigate the disinfection kinetics for practical purposes [13–15]. These studies have demonstrated that TiO_2-mediated photooxidation shows much promise for the elimination of microorganisms in many applications especially in the areas where the use of chemical cleaning agents or biocides has proven to be ineffective or is restricted by regulations, e.g., in the pharmaceutical or food industry. The photobiocide properties of TiO_2 also open the possibility of developing highly effective self-cleaning and self-sterilizing materials [16].

Although the bactericidal mode of TiO_2 photocatalysis was investigated mostly with the use of fine TiO_2 particles, this type of photocatalytic systems is only of limited practical importance because of the need of ultimate removing of highly dispersed photocatalyst from the treated solution by filtration or centrifugation. To overcome this drawback, many approaches were proposed including fabrication of magnetic photocatalysts [17,18], combination of nanocrystalline titania with the organic mesophases [7,19], etc.; however, the immobilization of photocatalyst on the conducting or nonconducting substrates still remains the most efficient approach to solving this problem regardless of some loss in the surface-to-volume ratio as compared to the photocatalyst suspensions.

The modification of titania particles or thin films with metal nanoparticles (first of all, with the particles of noble metals) is commonly used for the enhancement of the efficiency of photocatalysis. The metal deposits generally act as the sink for photoinduced charge carriers thus promoting interfacial charge-

* Corresponding author. Tel.: +375 296 38 49 39; fax: +375 172 102 101.
E-mail addresses: katjaskorb@mpikg.mpg.de, anok-skv@mail.ru (E.V. Skorb).

0926-3373/$ – see front matter © 2008 Elsevier B.V. All rights reserved.
doi:10.1016/j.apcatb.2008.03.007

transfer reactions [20–22] or improve the selectivity of the photoinduced reactions on the photocatalyst surface [23,24]. The antimicrobial tests have shown that silver-modified [25–27] and Ag_2O-loaded [28] TiO_2 films are very effective in preventing the colony formation in the case of both gram-negative and gram-positive bacteria. However, the exact role of metal deposition in the formation of antimicrobial abilities of metal-modified photocatalysts still remains unclear. Moreover, silver in the nanoparticulated form possesses its own microbiocide activity caused by prolonged oxidation of silver nanoparticles accompanied with the release of Ag^+ ions that opens fresh opportunities for developing of photocatalytic systems with the enhanced pathophysiological activity. In a similar manner, the cytotoxic activity of copper ions emitted during operation of copper-modified TiO_2 photocatalyst ensures its high bactericidal activity even under very weak UV light illumination [29].

In this work, bactericidal activities of nanostructured TiO_2 films modified with Ag and bimetallic Ag/Ni nanoparticles as well as TiO_2:In_2O_3 films, introduced recently as a highly effective nanocomposite photocatalysts [30,31], are investigated in killing of both gram-positive and gram-negative bacteria with the special reference on the role of the photoproduced reactive oxygen species of different types in the cell inactivation.

2. Experimental

Unless stated otherwise, all materials were purchased from Sigma–Aldrich Chemical Co. and used as supplied. The Milli-Q water was used for preparation of solutions.

The titanium dioxide and indium hydroxide sols used for deposition of the photocatalytically active coatings were obtained by controlled hydrolysis in combination with ultrasonic dispergation. For preparation of sols, 2.5 M $TiCl_4$ + 0.65 M HCl or 0.25 M $In(NO_3)_3$ aqueous solutions were slowly titrated with 12.5% NH_4OH under continuous mechanical stirring until the final pH of 5 (TiO_2) and 8 ($In(OH)_3$) was reached. The precipitate was then centrifuged, washed out with distilled water, and exposed to ultrasound (22 kHz). Before the sonication, HNO_3 was added as the stabilizer in an amount corresponding to the TiO_2:HNO_3 mole ratio of 5:1 and $In(OH)_3$:HNO_3 mole ratio of 20:1. For further details concerning synthesis of sols see Refs. [30,32].

Thin-film photocatalysts were prepared by spraying the sol of titanium dioxide or its mixture with indium hydroxide (weight ratio of 4:1) onto the glass microscope slides or glazed ceramic tiles heated to 200 °C. The concentration of sols used for deposition of photocatalysts was of 5 g/l. The resultant TiO_2 and TiO_2:In_2O_3 coatings were then annealed at 450 °C for 1.5 h in air. Before the photocatalyst deposition, the surface of the substrate was coated with a silicon dioxide blocking layer by spraying the aqueous sol of SiO_2 to prevent migration of sodium ions from a glaze during annealing (the latter factor could adversary affect the photoactivity of titania [33]). Thus obtained photocatalytic coatings were robust and resistant to scratch tests with a stainless steel spatula. The average diameter of TiO_2 crystallites (anatase) estimated from the half-width of the X-ray diffraction peaks was of ca. 7 nm for TiO_2 film and ca. 5 nm for TiO_2:In_2O_3 composite film, while the In_2O_3 crystallites were ca. 11 nm in size. According to the Rutherford backscattering spectra, the thickness of TiO_2 and TiO_2:In_2O_3 films was of ca. 0.2 μm.

Silver nanoparticles were deposited onto the TiO_2 film by UV light illumination of photocatalyst surface for 10 s in the contact with 10^{-5} M Ag_2SO_4 aqueous solution. Nickel caps were grown over silver nuclei via electroless deposition from hypophosphite plating bath of the following composition: 18 g/l $Ni(CH_3COO)_2$ + 37 g/l $Na_2H_2PO_2$ + 40 g/l $NaCH_3COO$, pH 6; the deposition temperature was of 55 °C and the deposition time was 30 s. Silver and nickel loadings, which were optimized so that to attain the highest photocatalytic activity, amount ca. 2×10^{15} Ag atoms/cm^2 and ca. 5×10^{14} Ni atoms/cm^2 as estimated from Rutherford backscattering spectra for TiO_2/Ag and TiO_2/Ag/Ni films.

The surface morphology of the photocatalysts was studied by scanning electron microscopy (SEM) (LEO-1420, Carl Zeiss, Germany) and atomic force microscopy (AFM) (Molecular Force Probe 1D AFM, Asylum Co., Santa Barbara, USA). The morphology of metal deposits was investigated by transmission electron microscopy (TEM) using LEO 906 E transmission electron microscope (Carl Zeiss, Germany) with accelerating voltage of 120 kV; samples for TEM were prepared by the extractive replica technique.

The photocatalytic activities of TiO_2, TiO_2/Ag, TiO_2/Ag/Ni, and TiO_2:In_2O_3 films were evaluated by the photodegradation of Rhodamine 6G. For these purpose, the thin-film photocatalyst deposited onto the bottom of the flat cell was illuminated through the thin layer of 5×10^{-6} M aqueous solution of probing dye. The decay of dye concentration during the illumination was followed photometrically.

Ultraviolet illumination was carried out using high-pressure mercury lamp Philips HPK 125 W equipped with 310–400 nm filter. The intensity of incident light was ~15 mW cm^{-2}. As the measure of the photoactivity, Y, we have used the relative drop of a dye concentration after 5 min of illumination.

The amount of superoxide generated at the water-photocatalyst interface under UV illumination was quantitatively determined using tetranitromethane, which is known to be a selective scavenger of $O_2^{\bullet -}$ [34]. For these purposes, the samples (the glass slides, 1 cm × 1 cm in size, with the thin-film photocatalysts deposited onto their surface) were placed at the bottom of quartz cuvette and illuminated under a thin layer of water with UV light for 10 min. Immediately after illumination, the tetranitromethane aqueous solution was added into the cuvette. An amount of nitroform, $C(NO_2)_3^-$, produced due to reduction of tetranitromethane by $O_2^{\bullet -}$ was evaluated photometrically (the extinction coefficient for $C(NO_2)_3^-$ is of 14,800 mol l^{-1} cm^{-1} at 350 nm [35]).

Photoelectrochemical measurements were performed under potentiostatic conditions (a conventional three-electrode scheme of polarization). The thin-film photocatalysts deposited onto the ITO glass plates were used as the working electrodes. The aqueous electrolyte employed was 0.25 M Na_2SO_4 with the addition of 0.1 M CH_3COONa as a hole scavenger. Potentials were measured against Ag/AgCl, Cl^-(sat.) reference electrode (0.201 V versus NHE).

The hydrophilic/hydrophobic properties of the thin-film photocatalysts were studied using Contact Angle Measurement System G10 (Krüss, Germany). A droplet of distilled water was placed on the photocatalyst surface and the water contact angle was then measured.

The antimicrobial activity of the samples was determined using gram-negative bacterium *Psedomonas fluorescens* B-22 and gram-positive bacterium *Lactococcus lactis* ssp. *lactis* 411 as the test-cultures. The overnight cultures in nutrient broth (*P. fluorescens*) or in peptone-yeast MRS medium (*L. lactis*) were diluted with sterile 0.15 M NaCl, then 900 μl of bacteria suspensions was placed in flat cells with a bottom made of ceramic tile onto which the thin-film photocatalysts were deposited; the control cell have no photocatalyst at the bottom. All cells were exposed to UV light for 10 min; after that the suspensions of microorganisms were placed on the nutrient agar media (in the case of *P. fluorescens*) or nutrient MRS media (in the case of *L. lactis*). Plates were incubated for 48 h under 30 °C and a colony number was calculated taking into account the dilution factor. The respective data were the average of values obtained from triplicate runs. The standard deviations of three replicate experiments were within 7%. The thin-film

photocatalysts under consideration have not shown a decrease in their photoinduced microbiocide efficiency when the antimicrobial experiments were repeated three times using the same samples (after each experiment samples were thoroughly washed with water). In the control test, when UV light was not applied, no inactivation of microorganisms was observed.

To evaluate the photoinduced biocide activity, the two parameters were calculated: (i) the survival ratio and (ii) the reduction factor. The survival ratio ($S = N/N_0 \times 100\%$, where N_0, N are the numbers of CFUs before and after UV light exposure, respectively) provides an information on the overall bactericidal efficiency of the photocatalytic systems under investigation. The reduction factor ($RF = N_c/N$, where N, and N_c are the numbers of CFUs remaining in suspension after UV light exposure in contact with photocatalytic coating and photocatalyst-free ceramic substrate, respectively) permits one to compare the efficiency of photocatalytic inactivation with that of photochemical one.

To evaluate the cell adsorption, the number of microorganisms remaining in the cell suspension equilibrated with the photocatalyst surface (the equilibrium is normally attained in 5–10 min) was measured and the adsorption efficiency, A, was calculated ($A = N_a/Ns_{a0}$, where N_{a0} and N_a are the numbers of CFUs before and after adsorption).

3. Results and discussion

The thin-film TiO_2 and TiO_2:In_2O_3 photocatalysts have an uniform surface which is free of cracks as evidenced by SEM microphotographs shown in Fig. 1. The values of root mean square roughness, R_{ms}, evaluated from AFM 1.0 μm × 1.0 μm surface plots point to the fact that TiO_2:In_2O_3 film exhibits more developed surface: the R_{ms} increases from 1.3 to 1.9 nm when going from TiO_2 to TiO_2:In_2O_3. The TEM investigations evidence that photocatalytic deposition of silver yields uniformly distributed silver nanoparticles with the medium size of ~2.5 nm. Electroless nickel deposition, which concentrates at silver centers, results in some increase of medium size of bimetallic particles (up to ~3.5 nm). Metal deposition enhances the surface roughness, which exhibits an increase up to 1.6 nm (TiO_2/Ag) and 1.7 nm (TiO_2/Ag/Ni).

The Rhodamine 6G photodegradation measurements have evidenced that TiO_2 film shows a pronounced photocatalytic activity (Table 1). Modification of TiO_2 surface by deposition of silver nanoparticles results in sharp increase in the photoactivity, the latter exhibiting only slight decrease upon nickel deposition over silver nuclei. The XPS studies show that Ag $3d_{5/2}$ photoelectron peak centered at 368.1 eV (that match exactly literature value for silver metal [36]) does not exhibit a shift to lower energies upon UV exposure in aqueous solution providing an evidence that silver nanoparticles does not suffer from oxidation during the course of photocatalytic experiment, i.e., the trapping of photoholes by surface hydroxyl groups and water molecules appears to be much more effective than the photohole trapping by silver deposition.

The results of the bactericidal activity performance studies are collected in Tables 2 and 3. Drastic decrease of the number of viable cells was observed for the illuminated TiO_2 film as compared to the substrate (glazed ceramic plate) that points to the pronounced photokilling ability of the nanostructured TiO_2 film. Modification of TiO_2 surface with Ag nanoparticles results in further enhancement of the photoinduced microbiocide efficiency: the *RF* value increases ca. 2-fold in the case of *P. fluorescens* and by 15% in the case of *L. lactis*. In contrast, the TiO_2/Ag/Ni photocatalyst demonstrates much lower photokilling efficiency as compared

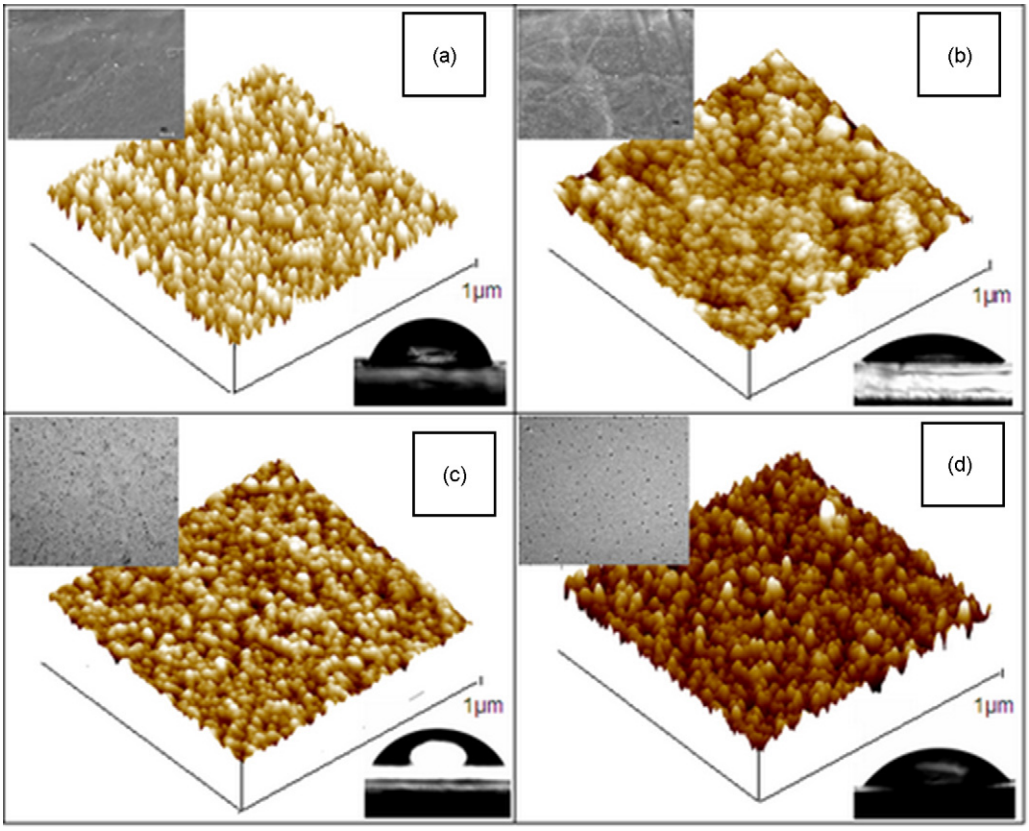

Fig. 1. AFM surface plots for: (a) TiO_2; (b) TiO_2:In_2O_3; (c) TiO_2/Ag; (d) TiO_2/Ag/Ni. Insets—left upper corner: SEM images of (a) TiO_2; (b) TiO_2:In_2O_3, TEM images of (c) Ag nanoparticles at TiO_2 surface; (d) Ag/Ni nanoparticles at the TiO_2 surface. Insets—right bottom corner: optical images of water drop on the surface of (a) TiO_2; (b) TiO_2:In_2O_3; (c) TiO_2/Ag; (d) TiO_2/Ag/Ni.

Table 1
Photocatalytic activity, efficiency of $^{\bullet}O_2^-$ photogeneration and contact angle values for thin-film photocatalysts

Photocatalytic surface	Y	I_s[a]	Contact angle (°)
TiO_2	0.19	1.0	72
TiO_2:In_2O_3	0.29	0.9	41
TiO_2/Ag	0.33	1.3	49
TiO_2/Ag/Ni	0.32	1.6	46
Ceramic substrate	0.15	0	80

[a] Superoxide yield is normalized to the superoxide production at the surface of bare TiO_2 (the amount of the superoxide generated at the TiO_2 surface under UV irradiation was of ca. 1.5×10^{15} superoxide ions per cm^2).

Table 2
The effect of UV irradiation on the survival of *P. fluorescens*

Illuminated surface	Number of viable cells after irradiation (CFU/ml)	S (%)	RF
TiO_2	3.6×10^1	0.05	33.3
TiO_2:In_2O_3	4.1×10^2	0.55	2.9
TiO_2/Ag	1.7×10^1	0.02	70.6
TiO_2/Ag/Ni	2.4×10^2	0.32	5.0
Ceramic substrate	1.2×10^3	1.62	1.0

Initial concentration of microorganisms 7.2×10^4 CFU/ml.

Table 3
The effect of UV irradiation on the survival of *L. lactis*

Illuminated surface	Number of viable cell after irradiation (CFU/ml)	S (%)	RF
TiO_2	2.8×10^2	0.82	16.1
TiO_2:In_2O_3	8.3×10^2	2.44	5.4
TiO_2/Ag	2.4×10^2	0.71	18.8
TiO_2/Ag/Ni	2.5×10^2	0.73	18.0
Ceramic substrate	4.5×10^3	13.23	1.0

Initial concentration of microorganisms 3.4×10^4 CFU/ml.

to TiO_2/Ag one, the decrease in the photoinduced microbiocide efficiency being especially pronounced for *P. fluorescens* (Tables 2 and 3). The photokilling activity also exhibits a decrease as one goes from TiO_2 to TiO_2:In_2O_3 (Tables 2 and 3). The observed

Table 4
Adsorption efficiency for *P. fluorescens* and *L. lactis*

Photocatalyst	A (%)	
	P. fluorescens	*L. lactis*
TiO_2	5.6	9.9
TiO_2:In_2O_3	7.8	11.9
TiO_2/Ag	32.6	31.5
TiO_2/Ag/Ni	21.3	25.2
Ceramic substrate	3.4	4.6

variations in the photoinduced antimicrobial activity poorly correlate with the activity of thin-film photocatalysts towards degradation of Rhodamine 6G in aqueous medium: TiO_2:In_2O_3 and TiO_2/Ag/Ni films demonstrating high photocatalytic activity, which is only slightly less then that of the most active TiO_2/Ag photocatalyst, exhibit the lowest bactericidal activity against test-cultures used (cf. Tables 1–3).

The cell adsorption measurements evidence that the number of adsorbed microorganisms exhibits drastic increase as the result of modification of TiO_2 surface with silver and Ag/Ni nanoparticles, whereas TiO_2:In_2O_3 film demonstrates only slight increase in the ability to adhere *P. fluorescens* and *L. lactis* bacteria (Table 4). The observed increase in the adsorption capacity cannot be attributed to enhanced hydrophilicity of metal-modified TiO_2 (the water contact angle decreases from 72° to 49° as one goes from TiO_2 to TiO_2/Ag) since TiO_2:In_2O_3 film is also highly hydrophilic (Table 1); the enhanced affinity of metal-modified titania to microorganisms can be rather attributed to the developed surface of these photocatalysts. The adhered bacteria are not fixed tightly to the surface of photocatalyst and can be readily washed out; the number of microorganisms remaining after brief rinsing with water, evaluated from optical images shown in Fig. 2, is of 3×10^4 cm^{-2}, this value being almost the same for all the photocatalysts under consideration.

The photocurrent measurements show that the deposition of silver nanoparticles results in the ca. 2-fold increase in the anodic photocurrent (Fig. 3) pointing to the lowering of the recombination

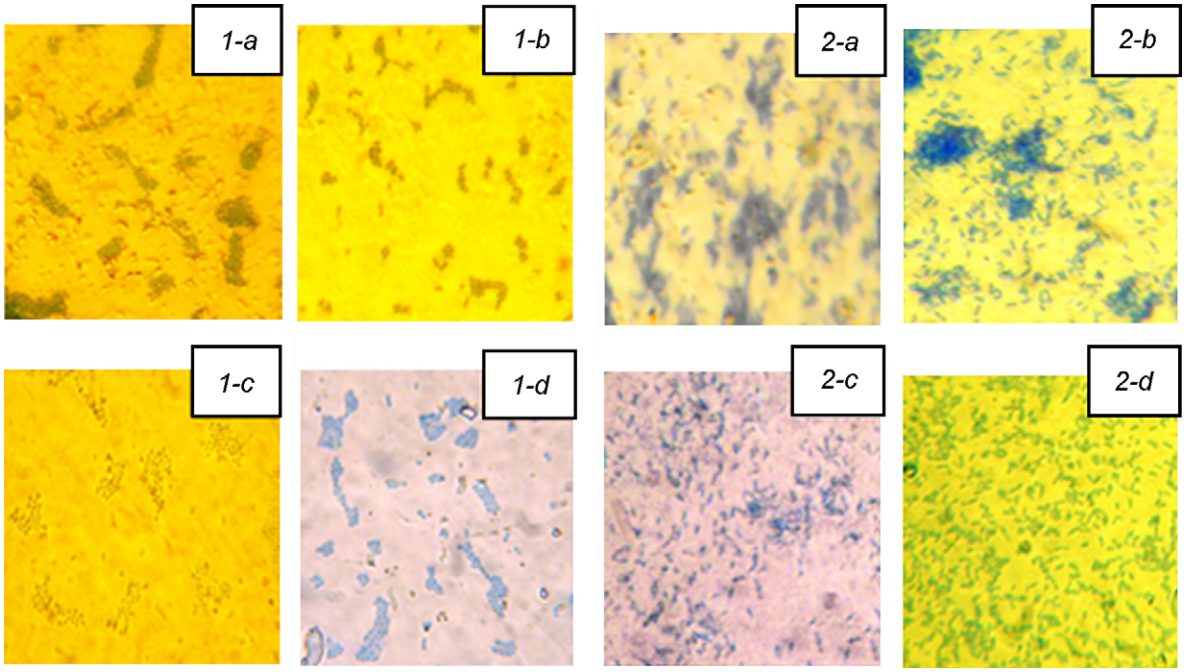

Fig. 2. Optical images of (1) *L. lactis* and (2) *P. fluorescens* adsorbed at: (a) TiO_2; (b) TiO_2:In_2O_3; (c) TiO_2/Ag; (d) TiO_2/Ag/Ni.

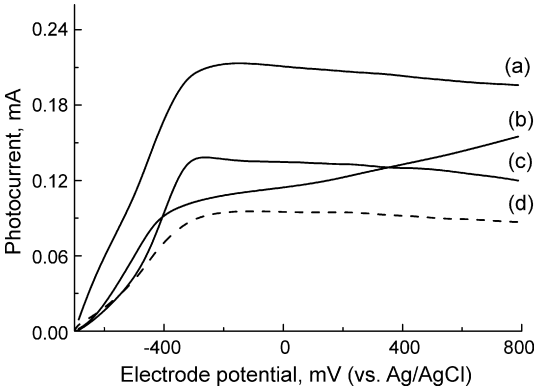

Fig. 3. Photocurrent versus potential curves for (a) TiO_2/Ag; (b) TiO_2/Ag/Ni; (c) TiO_2; (d) TiO_2:In_2O_3.

losses. The observed effect can be attributed to the metal-induced splitting of energy levels corresponding to the surface states in the forbidden zone of TiO_2 that suppresses the surface recombination of the photoproduced charges (the possibility of such alterations of the energy distribution of electronic states upon modification of the surface of TiO_2 with fine particles of noble metals was shown previously employing the electrolyte electroreflectance spectroscopy [37]). Higher efficiency of photogeneration of charge carriers agrees well with the observed enhancement of the superoxide yield for silver-modified TiO_2 films (Table 1). In contrast, nickel, having more negative potential of Me/Me^+ couple than that of silver, should produce surface states lying much deeper in the forbidden zone of TiO_2 [38]. These surface states are capable to facilitate the recombination that is consistent with the lower photocurrent values for TiO_2/Ag/Ni electrode than that for TiO_2/Ag electrode (Fig. 3). Since the hydroxyl radicals are generally much stronger cytotoxic agent than superoxide ions [39,40], the enhanced yield of $^{\bullet}O_2^-$ photoproduction in the case of TiO_2/Ag/Ni does not compensate the decrease in the charge separation efficiency upon nickel deposition over silver centers that results in low photobiocide efficiency against *P. fluorescens* inherent in this photocatalyst (Table 2); however, in the case of *L. lactis* the decrease in the reduction factor upon nickel deposition is minimal (Table 3) suggesting that superoxide effectively contributes in the inactivation of this bacterium. On the other hand, the photoproduced superoxide ions are involved in the photodegradation of Rhodamine 6G [30] resulting in high photocatalytic activity of TiO_2/Ag/Ni towards this probing dye (Table 1). Higher yield of superoxide in the case of TiO_2/Ag/Ni as compared to TiO_2/Ag points to the enhanced rate of disappearance of superoxide at the silver-modified TiO_2 surface, suggesting that superoxide radicals undergo further reactions to form hydroxyl radicals via the formation of hydrogen peroxide [41], these hydroxyl radicals being capable to participate in the bacteria inactivation. The latter fact can be responsible for extra high biocide activity demonstrated by TiO_2/Ag films.

It is seen from Tables 2 and 3 that TiO_2 and TiO_2/Ag photocatalysts show much higher activity against *P. fluorescens* than against *L. lactis*. This difference can be attributed to the differences in the cell wall structure inherent in gram-negative and gram-positive bacteria. Thus, *L. lactis* (gram-positive bacterium) possesses strong murein skeleton, more then 30 murein layers strengthened by inter-chain peptide bridges and molecules of teichoic acids. As the result, the thickness of *L. lactis* cell wall can reach 40 nm. In contrast, the cell wall of *P. fluorescens* (gram-negative bacterium) consists of just one thin (~2 nm) murein layer and membrane made of lipopolysaccharides, phospholipids and proteins. The fact that the highest efficiency of inactivation of *P. fluorescens* is attained in the case of TiO_2/Ag films, which ensure the most favorable conditions for generation of hydroxyl radicals, permits a conclusion that the envelop of *P. fluorescens* is rather resistant and exhibits degradation (at least at the initial stages the cell wall damage) only being attacked by hydroxyl radicals. The higher deactivation efficiency in the case of gram-negative bacteria as compared to gram-positive ones was reported earlier [13,42]. However, other studies have found gram-positive bacteria to be more sensitive than gram-negative bacteria to the antibacterial effects of TiO_2 [43]. It has been also shown that photoinactivation of gram-negative bacterium *E. coli* at the surface of Ag_2O-loaded TiO_2 film occurs with lower efficiency than photoinactivation of gram-positive bacteria *S. aureus* and *B. cereus* [28]. This permits a conclusion that the bacteria photoinactivation rate is governed not only by cell wall thickness but also by the morphology of cell envelop and resistance of outer membrane to the reactive oxygen species produced at the photocatalyst surface. The enhanced response of *P. fluorescens* as compared to *L. lactis* to the TiO_2 photocatalytic reactions can also be due to the differences in the metabolism of bacteria. Pseudomonades, being the obligate aerobes, store energy via the oxidative phosphorylation, with the motive force of the ATP synthesis being the proton gradient arising as the result of cell respiratory function. The increase in the ion permeability due to damage of the cytoplasmic membrane by reactive oxygen species capable to oxidize lipids results in the vanishing of the proton gradient that, in its turn, hinders the bacteria respiratory function. On the contrary, *L. lactis*, which is the facultative anaerobe, does not breathe and store energy in other metabolic process involving the lactic acid fermentation. Since the substrate-linked phosphorylation occurs in the cytosol, the effect of the damages in the cytoplasmic membrane in the case of *L. lactis* is not so noticeable like in the case of *P. fluorescens*.

4. Conclusions

The thin-film nanostructured photocatalysts TiO_2, TiO_2:In_2O_3, TiO_2/Ag, and TiO_2/Ag/Ni prepared at the ceramic substrates by spaying oxide sols with subsequent silver photodeposition and electroless nickel deposition were screened for their antibacterial efficiency against *P. fluorescens* and *L. lactis*. The highest photobiocide activity was found to be inherent in TiO_2/Ag film demonstrating the enhanced efficiency of cell adsorption (the adsorption increases 6-fold) and high yield of photoproduction of both hydroxyl radicals (the major lethal factor) and superoxide ions. Due to rather low silver loading (several monolayers), the pathophysiological properties of the TiO_2/Ag photocatalysts are solely due to the photocatalytic processes induced at their surface under UV light illumination. The photocatalysts show higher activity against *P. fluorescens* than *L. lactis* that can be explained in terms of different morphologies of gram-positive and gram-negative cell envelops.

Acknowledgement

This work was supported by the Basic Research Foundation of Belarus (grants X07-095, X07-175) and NATO Collaboration Linkage grant #CLG 982758.

References

[1] A. Fujishima, K. Honda, Nature 238 (1972) 37–38.
[2] A. Fujishima, T.N. Rao, D.A. Truk, J. Photochem. Photobiol. C: Photochem. Rev. 1 (2000) 1–21.
[3] D. Bahnemann, Solar Energy 77 (2004) 445–459.
[4] A.G. Agrios, P. Pichat, J. Appl. Electrochem. 35 (2005) 655–663.

[5] E. Kaneko, I. Okura (Eds.), Photocatalysis: Science and Technology, Springer, Berlin, 2003.
[6] A. Heller, Acc. Chem. Res. 28 (1995) 503–508.
[7] D.G. Shchukin, D.V. Sviridov, J. Photochem. Photobiol. C: Photochem. Rev. 7 (2006) 23–26.
[8] M.R. Hoffmann, S.T. Martin, W. Choi, D.W. Bahnemann, Chem. Rev. 95 (1995) 69–96.
[9] T. Matsunaga, T. Tomoda, N. Nakajima, H. Wake, FEMS Microbiol. Lett. 29 (1985) 211–216.
[10] Z. Huang, P.-C. Maness, D.M. Blake, E.J. Wolfrum, S.L. Smolinski, W.A. Jacoby, J. Photochem. Photobiol. A: Chem. 130 (2000) 163–170.
[11] P. Amezaga-Madrid, R. Silveyra-Morales, L. Cordoba-Fierro, G.V. Nevarez-Moorillon, M. Miki-Yoshida, E. Orrantia-Borunda, F.J. Solis, J. Photochem. Photobiol. B. 70 (2003) 45–50.
[12] J.M. Robertson, P.K. Robertson, L.A. Lawton, J. Photochem. Photobiol. A: Chem. 175 (2005) 51–56.
[13] A.-G. Rincón, C. Pulgarin, Appl. Catal. B: Environ. 49 (2004) 99–112.
[14] B. Kim, D. Kim, D. Cho, S. Cho, Chemosphere 52 (2003) 277–281.
[15] J.A. Ibáñez, M.I. Litter, R.A. Pizarro, J. Photochem. Photobiol. A: Chem. 157 (2006) 81–85.
[16] N.P. Mellott, C. Durucan, C.G. Pantano, M. Guglielmi, Thin Solid Films 502 (2006) 112–120.
[17] D.G. Shchukin, A.I. Kulak, D.V. Sviridov, Photochem. Photobiol. Sci. 1 (2002) 742–744.
[18] J. Rawat, S. Rana, R. Srivastava, R.D.K. Misra, Mater. Sci. Eng. C. 27 (2007) 540–546.
[19] D.G. Shchukin, E.A. Ustinovich, A.I. Kulak, D.V. Sviridov, Photochem. Photobiol. Sci. 3 (2004) 157–159.
[20] K. Hirano, H. Asayama, A. Hoshino, H. Wakatsuki, J. Photochem. Photobiol. A: Chem. 110 (1997) 307–311.
[21] J. He, P. Yang, H. Sato, Y. Umemura, A. Yamagishi, J. Electroanal. Chem. 566 (2004) 227–233.
[22] S. Sen, S. Mahanty, S. Roy, O. Heintz, S. Bourgeois, D. Chaumont, Thin Solid Films 474 (2005) 245–249.
[23] D. Shchukin, E. Ustinovich, D. Sviridov, P. Pichat, Photochem. Photobiol. Sci. 3 (2004) 142–144.
[24] H. Tran, J. Scott, K. Chiang, R. Amal, J. Photochem. Photobiol. A: Chem. 183 (2006) 41–52.
[25] M. Bekbolet, Water Sci. Technol. 35 (1997) 95–97.
[26] M.P. Reddy, A. Venudopal, M. Subrahmanyam, Water Res. 41 (2007) 379–386.
[27] G. Gogniat, M. Thyssen, M. Denis, C. Pulgarin, S. Dukan, FEMS Microbiol. Lett. 258 (2006) 18–24.
[28] K. Page, R.G. Palgrave, I.P. Parkin, M. Wilson, S.L.P. Savin, A.V. Chadwick, J. Mater. Chem. 17 (2007) 95–104.
[29] K. Sunada, T. Watanabe, K. Hashimoto, Environ. Sci. Technol. 37 (2003) 4785–4789.
[30] E.V. Skorb, E.A. Ustinovich, A.I. Kulak, D.V. Sviridov, J. Photochem. Photobiol. A: Chem. 193 (2008) 97–103.
[31] A.S. Deshpande, D.G. Shchukin, E.A. Ustinovich, M. Antoniette, R.A. Caruso, Adv. Funct. Mater. 15 (2005) 239–246.
[32] D. Shchukin, S. Poznyak, A. Kulak, P. Pichat, J. Photochem. Photobiol. A: Chem. 162 (2004) 423–430.
[33] H. Tada, M. Tanaka, Langmuir 13 (1997) 360–364.
[34] K. Ishibashi, A. Fujishima, T. Watanabe, K. Hashimoto, J. Phys. Chem. B. 104 (2000) 4934–4946.
[35] J. Rabani, W.A. Mulac, M.S. Maseson, J. Phys. Chem. 69 (1965) 53–57.
[36] S.W. Gaarenstroom, N. Winograd, J. Chem. Phys. 67 (1977) 3500–3506.
[37] A.I. Kulak, A.I. Kokorin, D.V. Sviridov, J. Mater. Res. 16 (2001) 2357–2362.
[38] A.I. Kulak, in: A. Kokorin, D. Bahnemann (Eds.), Chemical Physics of Nanostructured Semiconductors, VSP, Utrecht, 2003, pp. 153–182.
[39] M. Cho, H. Chung, W. Choi, J. Yoon, Appl. Environ. Microbiol. 71 (2005) 270–275.
[40] P.-C. Maness, S. Smolinski, D.M. Blake, Z. Huang, E.J. Wolfrum, W.A. Jakoby, Appl. Environ. Microbiol. 65 (1999) 4094–4098.
[41] A. Vamathevan, R. Amal, D. Beydoun, G. Low, S. McEvoy, Chem. Eng. J. 98 (2004) 127–139.
[42] A. Pal, S.O. Pehkonen, L.E. Yu, M.B. Ray, J. Photochem. Photobiol. A: Chem. 186 (2007) 335–341.
[43] G. Fu, P.S. Vary, C.-T. Lin, J. Phys. Chem. B. 109 (2005) 8889–8898.